NeuroImage 188 (2019) 188–197

Contents lists available at ScienceDirect

NeuroImage

journal homepage: www.elsevier.com/locate/neuroimage

Hemodynamic and neuronal responses to cocaine differ in awake versus anesthetized animals: Optical brain imaging study

Kicheon Park [a], Wei Chen [a,1], Nora D. Volkow [b], Craig P. Allen [a], Yingtian Pan [a], Congwu Du [a,*]

[a] Department of Biomedical Engineering, Stony Brook University, Stony Brook, NY, 11794, USA
[b] National Institute on Alcohol Abuse and Alcoholism, National Institutes of Health, Bethesda, MD, 20857, USA

ARTICLE INFO

Keywords:
Vasoconstriction
Isoflurane
Cerebral blood flow
Oxygenated hemoglobin
GCaMP6f
Addiction
Neuronal $[Ca^{2+}]_i$ activity
Neuronal synchronization
Neurovascular coupling

ABSTRACT

Cocaine is a highly addictive drug with complex pharmacological effects. Most preclinical imaging studies investigating the effects of cocaine in the brain have been performed under anesthesia, which confounds findings. To tackle this problem, we used optical imaging to compare the effects of cocaine in the awake versus the anesthetized states. For this purpose, we customized an air floating mobile cage to fit the multi-wavelength spectral and laser speckle optical imaging system and implanted a multi-layer cranial window over the mouse somatosensory cortex. Results showed significant differences in neuronal activity and hemodynamics at baseline and in response to cocaine between the awake and the anesthetized states (isoflurane anesthesia). Specifically, 1) at baseline isoflurane dilated cerebral vessels, increased cerebral blood flow and depressed neuronal Ca^{2+} activity compared to the awake state; 2) acute cocaine (1 mg/kg iv) vasoconstricted blood vessels (arteries and veins) and decreased cerebral blood flow and oxygenated hemoglobin in the anesthetized state but not in the awake condition; 3) cocaine increased the accumulation of mean intracellular Ca^{2+} in neurons in the anesthetized state but not in the awake condition; and 4) in the awake state acute cocaine increased neuronal activities (increased the frequency of Ca^{2+} transients) and increased neuronal synchronization. We also corroborated that in the awake state cocaine also disrupted neurovascular coupling. These findings indicate that both vascular and neuronal responses to cocaine are influenced by isoflurane anesthesia, which highlights the importance of imaging awake animals when studying the effects of cocaine or other drugs in the brain.

1. Introduction

Cocaine is a highly addictive drug with adverse physiological effects (Center for Behavioral Health Statistics and Quality, 2016). In particular, the vasoconstricting effects of cocaine (Ren et al., 2012) reduce cerebral blood flow (CBF) (Volkow et al., 1988) and increase the risk for cerebrovascular accidents in those who consume it (Treadwell and Robinson, 2007, Desai et al., 2017). In animal models chronic exposure to cocaine can also trigger cerebrovascular accidents associated with cocaine's vasoconstricting effects (Ren et al., 2012; You et al., 2017).

In rodents anesthetized with isoflurane, we reported that acute cocaine triggered vasoconstriction of cerebral blood vessels (Park et al., 2015), reduced CBF (You et al., 2017), decreased the concentration of oxygenated hemoglobin in the somatosensory cortex (SSC) (Zhang et al., 2016) and disrupted neurovascular coupling (Chen et al., 2016a,b). However, we also observed that the anesthetic used influenced the hemodynamic responses to cocaine. For example, when rats were imaged under α-chloralose, acute cocaine temporarily increased CBF in the cortex whereas CBF was decreased under isoflurane (Du et al., 2009). In addition, others had shown that the neuronal effects of cocaine were sensitive to the anesthetic applied. For example, rats anesthetized with isoflurane had greater Fos expression in the frontal cortex following a cocaine challenge than rats anesthetized with α-chloralose (e.g. Kufahl et al., 2009). Moreover, the pharmacokinetics and specific binding of cocaine in the rat brain as assessed with positron emission tomography (PET) and [^{11}C]cocaine differed for isoflurane (faster clearance and higher specific to non-specific binding) than for α-chloralose (Du et al., 2009). These findings highlight the importance of studying the effects of cocaine (as well as that of other drugs) in the awake brain to obviate the confounding effects from the interaction of cocaine with the anesthetic

* Corresponding author. Department of Biomedical Engineering, State University of New York at Stony Brook, Life Science Bldg, Rm. 002, Stony Brook, NY, 11794-5281, USA.
E-mail address: Congwu.Du@stonybrook.edu (C. Du).
[1] Current address: Department of Physics, UC Berkeley, Li Ka Shing Center, Berkeley, CA 94720, USA.

https://doi.org/10.1016/j.neuroimage.2018.11.062
Received 18 July 2018; Received in revised form 29 October 2018; Accepted 30 November 2018
Available online 1 December 2018

agent.

To tackle this problem, we developed an optical technique to image the brain in the awake mouse that allowed us to measure the vasculature and hemodynamics in the cortex and by combining it with a genetically-encoded calcium indicator expressed in cortical neurons, to simultaneously measure neuronal activity. This allowed us to investigate the effects of acute cocaine on neuronal $[Ca^{2+}]_i$ (including mean neuronal $[Ca^{2+}]_i$ and $[Ca^{2+}]_i$ transients) along with the hemodynamic changes in the somatosensory cortex and to compare these responses between the awake and anesthetized state (with isoflurane). We hypothesized that cocaine-induced hemodynamic changes (i.e., oxygenated hemoglobin (HbO_2) and blood flow velocity (CBFv)) in the cortex would be attenuated in the awake compared to the isoflurane anesthetized state but that neuronal effects (neuronal $[Ca^{2+}]_i$) would be enhanced in the awake compared to the anesthetized state.

2. Material and methods

2.1. Animals

C57BL mice of 6–8 weeks old were used (n = 12; 6 male, 6 female). Animals were kept on a 12:12hr light cycle, with ad libitum access to food and water throughout the study. All experimental procedures were approved by the Institutional Animal Care and Use Committee of Stony Brook University.

2.2. Surgery and animal training

2.2.1. Viral injection

To measure neuronal activity mice were injected with a virus expressing the fluorescent intracellular calcium ($[Ca^{2+}]_i$) indicator, GCaMP6f (AAV1-Syn-GCaMP6f-WPRE-SV40) (PENN Vector Core). GCaMP6f was selected because of its stable expression and negligible bleaching for imaging (Lin and Schnitzer, 2016, Chen et al., 2013). All surgical tools were pre-sterilized by autoclave. Mice were mounted on stereotaxic (Kopf. Model 942) under anesthesia (~2.0% isoflurane in O_2). A small hole was drilled (Foredom K.1070) into the skull over the somatosensory cortex (A/P −2.0, M/L −2.0), and ~0.4ul of GCaMP6f was infused 400 μm below the brain surface (HAMILTON 65458-1). The virus was infused slowly for ~20 min and the injector was left in place for 15 min to allow for complete absorption by the brain tissue. After the injection, the animals recovered for 3 weeks to allow for the expression of GCaMP6f in neurons and were then implanted with a cranial window for repeated imaging.

2.2.2. Cranial window

A multi-layer cover-glass (inner layer: 0.3 mm, outer layer: 0.15 mm) was prepared before the surgery by cutting two pieces of 2 × 2 mm (inner layer) and one piece of 4 × 4 mm (outer layer) (Fisherbrand, Microscope cover glass, 12–540-B), then attaching the three layers with UV-curing optical adhesive (THORLABS Norland 68) (Goldey et al., 2014). Three weeks post GCaMP virus injection, the multi-layer cover glass was implanted ensuring that the gap between the removed-skull and the brain was filled up to immobilize the brain tissue and minimize motion artifacts during imaging. Specifically, a 2.5 × 2.5 mm cranial window was created over the SSC region (A/P −2.0, M/L-2.0) and the inner layer of the cover glass (2 × 2 mm) was pressed into the cranial window and attached to the brain surface. Two micro screws (Component supply co. MX-0090-01SP) were attached to the side of the skull, and the head-plate was affixed above the window. All components were secured with dental cement (H.E. Parmer Co. Inc., MIA622) (Goldey et al., 2014).

2.3. Mobile cage (treadmill)

For in vivo imaging, the mouse was placed in a custom 'floating cage' (treadmill) to allow us to image an awake moving animal. This cage was constructed from a light carbon fiber (ACP Co. cage wall: CFL-TW-10-1, cage bottom: CFL-TW-15R) and placed on an air table, which floated the cage approximately 0.7 mm above the table surface when activated (Supplemental Fig. S1 A). Since the cage floor shifted when the mouse attempted to walk, it created the illusion of free movement for the mouse while keeping the position of its head stationary (Kislin et al., 2014). Thus, head movement was minimized by the head fixation. The platform and cage assembly was mounted under the image probe of our custom multi-modality optical imaging platform (MIP). A transitional head holder, consisting of cross bars (McMaster, 8364T7) fixed with head-plate between the floating cage and the MIP, was used to quickly and accurately position the mouse head for imaging. For comparisons between the anesthetized and awake states, a custom isoflurane nose-piece was attached to the animal head holder to ensure stable anesthesia.

2.4. Training

To habituate the animals to the imaging procedure and minimize motion artifacts, animals were trained under the same condition as when imaged in the awake state. Supplemental Fig. S2 summarizes the timeline for animal training. Two-day training was conducted using procedures reported elsewhere (Tran and Gordon, 2015) but with extended, multiple training sessions, which included: 1) placing the animal on the air floating mobile cage and mounting the head-plate to a fixed-frame on the image stage to stabilize the relative position between the animal's head and the imaging probe, and 2) turning the light source to deliver the light through the cranial window using a time-sharing scheme to ensure multi-channel light exposure to simulate the imaging condition. The detailed training protocol is illustrated in Supplemental Fig. 2 (Inset plot), indicating how the training time was progressively increased from 5 min in the beginning to 10, 20, and 40 min with 10 min breaks between training sessions. To isolate from extraneous stimuli (Dombeck et al., 2007), we draped the imaging probe area with black cloth and turned off all the lights in the lab to minimize ambient visual and sound stimulations. We corroborated that the animals were properly trained and presented no obvious signs of stress during the awake imaging sessions based on visual inspection of their behaviors (e.g. vocalization and tendencies of motion) (Kislin et al., 2014; Madularu et al., 2017).

2.5. Multi-modality optical imaging of brain in vivo

In this study, we targeted imaging at week 4 post viral transfection since we recently showed that a 4–5 week period post viral transfection period provides the maximal neuronal Ca transients over background fluorescence signal (Gu et al., 2018). Specifically, in week 3 after viral injection of GCaMP6f, we prepared animals, including surgery for cranial window, head-plate implantation and animal training as per Supplemental Fig. S2, followed by optical imaging in week 4. A custom multi-modality optical imaging platform (Yuan et al., 2011) that combined fluorescence imaging, optical intrinsic signal imaging (OISI) and laser speckle contrast imaging (LSCI) was used to simultaneously detect neuronal Ca^{2+} and hemodynamic changes in the mouse cortex. As illustrated in Fig. 1b, three LEDs at the wavelengths of $\lambda_{HbT} = 568$ nm, $\lambda_{HbR} = 630$ nm and $\lambda_{Excitation} = 488$ nm (Spectra Light Engine, Lumicor) and one laser diode at $\lambda_{CBFv} = 830$ nm (DL8142-201-830, Thorlab) illuminated the cortical surface for hemodynamic and fluorescence imaging and for LSCI imaging of the relative cerebral blood flow velocity change (ΔCBFv). A scientific camera (sCMOS) was synchronized with the 4 illumination channels via an a data acquisition card (PCI-6221, National Instrument) for sequential image acquisitions with 10 ms exposure per channel (Chen et al., 2016a,b). Two different animal imaging protocols were used for the in vivo experiments. One imaging protocol was designed to track the hemodynamic and neuronal Ca^{2+} changes before and after cocaine, during which the changes in oxygenated-(ΔHbO_2), deoxygenated-hemoglobin (ΔHbR), cerebral blood flow velocity (ΔCBFv), vesicular diameter and neuronal $[Ca^{2+}]_i$ fluorescence (ΔF) as a

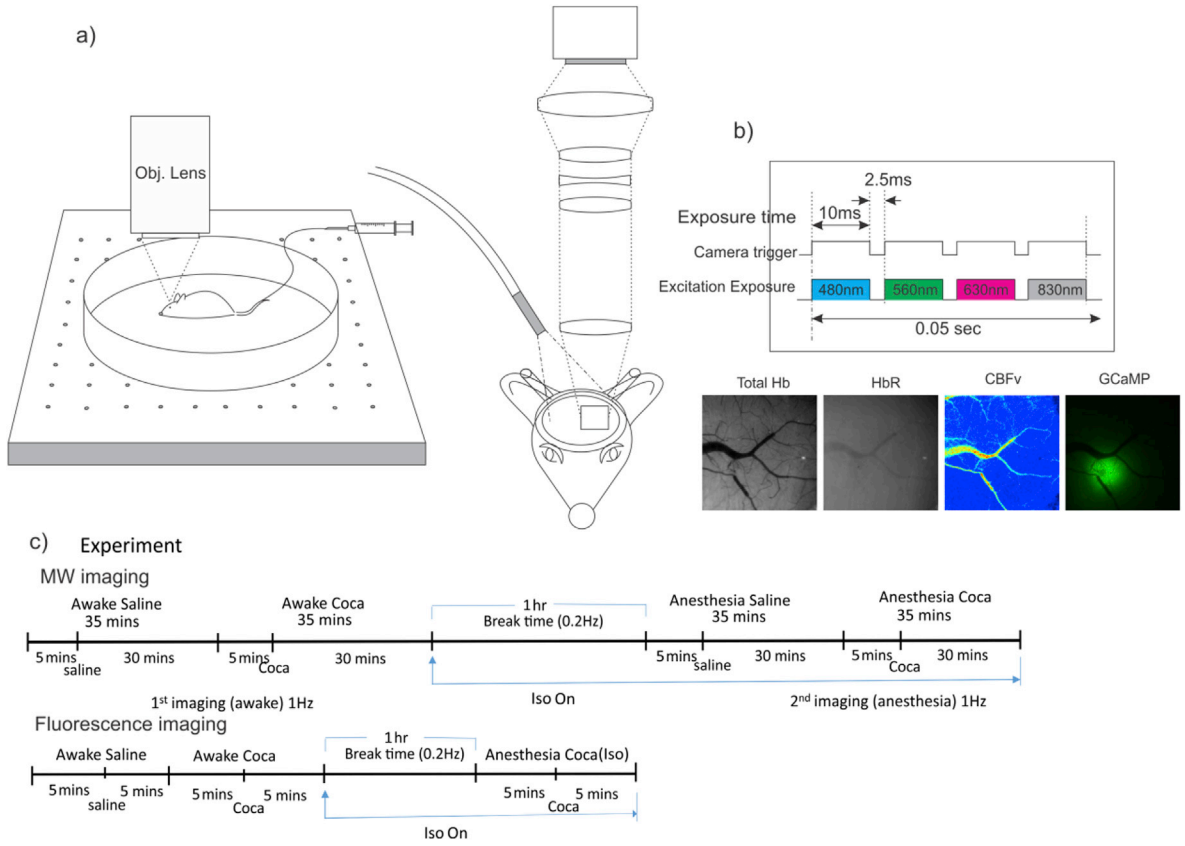

Fig. 1. A schematic illustrating custom multimodality optical imaging platform (MIP) for simultaneous GCaMP fluorescence and hemodynamic imaging and the image acquisition protocol. **a)** MIP with air-floating mobile cage; **b)** Time sharing scheme for light engine and camera to capture changes in Ca^{2+} fluorescence (GCaMP ΔF/F, 480nm/532 nm), total hemoglobin (ΔHbT, 560 nm), deoxygenated hemoglobin (ΔHbR, 560nm/647 nm), and ΔCBFv (830 nm) in vivo in mouse brain. **c**) Experimental protocol.

function of time were obtained. To accommodate long period tracking of brain status changes before and after cocaine, image acquisition was performed at 1 frame per second (1 fps or 1 Hz) for each channel over 40 min, i.e., 5min baseline followed by 35min after cocaine injection (1 mg/kg i.v.). The other imaging protocol aimed at investigating the rapid neuronal $[Ca^{2+}]_i$ transients, only single-channel fluorescence imaging (i.e., ΔF/F) was performed at 80 Hz for a total of 5min, including 2 min at baseline and 3min post cocaine injection (1 mg/kg, i.v.).

To compare the differences in cocaine-induced neuronal $[Ca^{2+}]_i$ and hemodynamic changes between the awake and anesthetized states, 2 sequential injections of cocaine (1 mg/kg iv per injection) were administrated 1hr apart to allow for the clearance of cocaine from brain and to restore the physiological condition to baseline levels. To switch from the awake to the anesthetized conditions, mice were given 2% isoflurane (Supplemental Fig. S1B) and maintenance of anesthesia was confirmed by a lack of pain response and stable breathing rates (Small Animal Instrumentation Inc, Model 1025L). Saline injections (0.1 ml) were used in the control group for comparison. For each animal, we compared the effects of acute cocaine for neuronal Ca^{2+} and hemodynamic changes in awake versus anesthetized conditions.

2.6. Data analysis

We first applied open-source image stabilization plugin function in Image J to all of the image stacks for minor motion correction and for image registration from frame to frame. We then split the 4-channel image stacks and performed post image processing to characterize the hemodynamic and $[Ca^{2+}]_i$ fluorescence changes. The changes in intracellular $[Ca^{2+}]_i$, vessel diameter (ΔØ), ΔHbT, ΔHbR, and ΔCBFv were quantified as percentage change relative to the baseline. For instance, ΔHbO_2(%) was derived by (Dunn et al., 2003; Luo et al., 2009):

$$\begin{bmatrix} \Delta HbO_2 \\ \Delta HbR \end{bmatrix} = \begin{bmatrix} \varepsilon^{\lambda_1}_{HbO_2} & \varepsilon^{\lambda_1}_{HbR} \\ \varepsilon^{\lambda_2}_{HbO_2} & \varepsilon^{\lambda_2}_{HbR} \end{bmatrix}^{-1} \times \begin{bmatrix} \ln\left(\frac{R_{\lambda_1}(0)}{R_{\lambda_1}(t)}\right) \Big/ L_{\lambda_1}(t) \\ \ln\left(\frac{R_{\lambda_2}(0)}{R_{\lambda_2}(t)}\right) \Big/ L_{\lambda_2}(t) \end{bmatrix} \quad (1)$$

where the molar extinction coefficients (ε) refer to the molar spectral absorptivities of the chromophores, i.e., HbO_2 and HbR. As ε is wavelength dependent, $\varepsilon^{\lambda_1}_{HbO_2}$, $\varepsilon^{\lambda_1}_{HbR}$, $\varepsilon^{\lambda_2}_{HbO_2}$, $\varepsilon^{\lambda_2}_{HbR}$ represent the extinction coefficients of these two chromophores at $\lambda_1 = 568$ nm and $\lambda_2 = 630$ nm $R_{\lambda_1}, R_{\lambda_2}$ are the diffuse reflectance at two wavelengths, and L_{λ_1} and L_{λ_2} are estimated pathlengths of light propagation (Dunn et al., 2005, Jacques, 2013). ANOVAs and multiple comparisons, using Bonferroni correction, were performed using SigmaStat software.

The mean $[Ca^{2+}]_i$ fluorescence was calculated by extracting multi-ROIs (~10 ROIs; 50–350 μm of diameter each) in brain regions with apparent fluorescence and free of large blood vessels. Additionally, ~6 ROIs were extracted away from the viral injection spot to compensate for the influence of cocaine-induced blood absorption changes (e.g., ΔHbT) on the measured GCaMP fluorescence emission (Yuan et al., 2011; Gu et al., 2018). The fluorescence intensity changes of individual neurons (i.e. $\Delta F_i(t)/F$) were measured and the neuronal activity frequencies (numbers of fluorescent Ca^{2+} transients, i.e., $\Delta F_i(t)/F$ per second) were quantified based on the intensity change patterns. Then, mixed-model analysis of variance (ANOVA) was applied to determine significant differences between groups and changes over time, multiple comparisons were performed using Bonferroni correction.

All statistical analyses were performed with Sigma Stat (Systat Software) with $p < 0.05$ for significance. Frequency spectrum of neuronal

Ca^{2+} transients was determined by Fast Fourier transform (FFT) and short-time Fourier transform (STFT) to characterize the frequency distribution of spontaneous neuronal activities and their changes with time (Chen et al., 2018). Neuronal activities in the frequency domain were analyzed and fitted as a Gaussian distribution to determine the full-width half-maximum (FWHM) bandwidth of the neural activities before and after cocaine to assess whether synchronization of neuronal activity was affected by cocaine.

3. Results

3.1. Isoflurane induced dilation in arteries and veins, increased blood flow and decreased neuronal Ca^{2+}

Fig. 2a shows representative images of the vascular network obtained from the cortex (top panels) and the dynamic map of their corresponding CBFv changes (bottom panel) before (t = −2min, a_0) and after isoflurane induction (t = 4min in a_1 t = 16min in a_3), in which the red and blue arrows identify the selected regions of interest (ROIs) for arteries and veins. To determine the effects of isoflurane on vessel diameter, we tracked the time-lapse diameter changes of veins (blue curve) and arteries (red curve) before and after induction of isoflurane (Fig. 2b_1-b_4). An one-way repeated measure ANOVA on the vein's diameter showed a significant time effect [$F(11,33) = 20.76$, $p < 0.001$] (N = 16; n = 4, ROIs = 4/animal). Multiple comparisons showed that diameters of veins increased from 30.31 ± 6.5 μm to 40.1 ± 7.3 μm ($p < 0.001$) at 25 sec after anesthesia and stabilized at 37.8 ± 7.4 μm ($p < 0.001$) after 125 sec, reflecting an average diameter increase of Δϕ = 26.73 ± 8.1%. Similarly, one-way repeated measure ANOVA showed a significant effect of time on the arteries diameter [$F(11,33) = 29.92$, $p = 0.002$] (N = 16; n = 4, ROIs = 4/animal). Multiple comparisons showed that arteries dilated from 14.65 ± 0.35 μm to 24.0 ± 2.68 μm at 25 sec after anesthesia ($p < 0.001$) and stabilized at 25.38 ± 1.8 μm ($p < 0.001$) with an average diameter increase of Δϕ = 66.8 ± 13.56% after 125 s. Repeated measure ANOVA also found that isoflurane increased CBFv in veins [$F(11,33) = 4.93$, $p < 0.001$] (N = 16; n = 4, ROIs = 4/animal) for nearly 100 s. Specifically, CBFv in veins significantly increased to 72.9 ± 42.1% from baseline after 50 s of isoflurane induction ($p = 0.02$) and peaked to 78.43 ± 34.17% at 75 s ($p = 0.01$). Isoflurane also increased CBFv in arteries [$F(11,33) = 5.46$, $p < 0.001$] (N = 16; n = 4, ROIs = 4/animal) for around 200 s (Fig. 2b_3). Multiple comparison showed CBFv in arteries increased to 138.34 ± 42.9% from baseline at 25 s after isoflurane induction and peaked to 181.52 ± 42.12% at 50 s ($p < 0.001$). A comparison of the changes at 3min after isoflurane revealed a significant difference between diameter increases in arteries (60.9 ± 13.69%) and in veins (27.31 ± 7.2%) [$F(1,3) = 7.37$, $p = 0.01$] (Fig. 2b_2) and between CBFv increases in arteries (118.42 ± 38.25%) and in veins (63.37 ± 25.36%) [$F(1,3) = 23.38$, $p = 0.013$] (Fig. 2b_4).

In the above study, awake recordings preceded those in the anesthetized state. To evaluate whether the order influenced CBFv, we measured CBFv(t) before, during, and after the interruption of isoflurane anesthesia (Supplemental Fig. S1B). The results showed that the transition of the changes in CBFv between the awake to the anesthetized stated occurred within ~1min and that upon interruption of isoflurane CBFv fully recovered to its baseline pre-anesthetic levels within 1min. This indicates that isoflurane-induced hemodynamic changes were transient and had no lingering effects.

Meanwhile, isoflurane significantly decreased neuronal [Ca^{2+}] fluorescence in cortex [$F(23,207) = 968.35$, $p < 0.001$], including mean Ca^{2+} fluorescence (F) and the Ca^{2+} activity change (ΔF(t)) (Fig. 2c_0). Specifically, F decreased −23.31 ± 2.89% from 1905.72 ± 56.5 a.u. to 1309.95 ± 723.2 a.u. ($p < 0.001$) within 40 s and stabilized at 1284.16 ± 383.1 a.u. or reduced −67.7 ± 6.1% after 5 min ($p < 0.001$, n = 4; Fig. 2d_1). Additionally, there was a reduction in ΔF(t) from awake to anesthetized state [$F(1,9) = 28.029$, $p < 0.001$]. If expressed as the relative Ca^{2+} fluorescence change, i.e., ΔF(t)/F decreased from

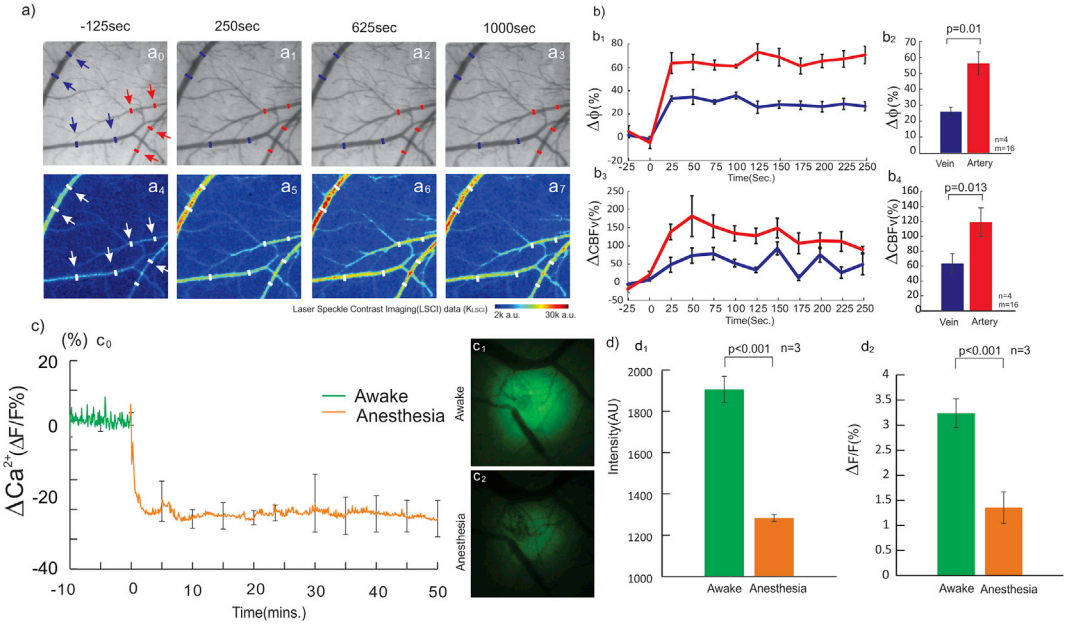

Fig. 2. Isoflurane dilates vessels, increases CBFv, and decreases neuronal mean $[Ca^{2+}]_i$. **a)** Time-lapse images of vessel diameters Δϕ (**a_0-a_3**) and ΔCBFv(**a_4-a_7**) in arteries and veins before and after isoflurane exposure (1.5–2%). **b_1)** Vasodilation after isoflurane, 26.73 ± 8.1% for veins [$F(11,33) = 20.76$, $p < 0.001$] and 66.8 ± 13.5% [$F(11,33) = 29.92$, $p = 0.002$] for arteries at 125 s. **b_2)** At 3min after isoflurane, vasodilation was different between veins and arteries [$F(1,3) = 7.37$, $p = 0.01$]. **b_3)** CBFv increased 72.92 ± 42.1% in veins [$F(11,33) = 4.93$, $p < 0.001$] and 181.52 ± 42.12% in arteries [$F(11,33) = 5.46$, $p < 0.001$] at 50 s after isoflurane, which returned to baseline at 100 s for veins and at 200 s for arteries. **b_4)** At 3min, CBFv increase was different between veins and arteries [$F(1,3) = 23.38$, $p = 0.013$]. **c_0)** Neuronal Ca^{2+} fluorescence abruptly decreased −23.31 ± 2.87% [$F(23,207) = 968.35$, $p < 0.001$] after 40sec after isoflurane and stabilized after 5min. **c_1-c_2)** $[Ca^{2+}]_i$ fluorescence images in awake and anesthetized states. **d_1)** Mean $[Ca^{2+}]_i$ in mouse cortex decreased in awake and anesthetized states after isoflurane ($p < 0.001$). **d_2)** Neuronal $[Ca^{2+}]_i$ fluctuation (ΔF(t)/F) decreased ($p < 0.001$) from 3.23 ± 0.3% in awake state (at t = −10 to 0min) to 1.3 ± 0.3% in isoflurane anesthetized state (at t = 40–50min).

3.23 ± 0.2% in awake state (t = −10 to 0 min; Fig.2c) to 1.36 ± 0.31% in anesthetized state (i.e., from t = 40–50 min; Fig. 2c), which indicates that isoflurane anesthesia reduced neuronal Ca^{2+} activity.

3.2. Cocaine induced vasoconstriction in anesthetized but not in awake mice

Fig. 3 shows cocaine-induced vessel diameter changes (t = 0, 1 mg/kg iv) in arteries (red curve & bar) and veins (blue curve & bar) in the anesthetized (Fig. 3a) and awake (Fig. 3b) states. In the anesthetized state (n = 4) cocaine significantly reduced the diameter of veins [F(147,49) = 3.39, p < 0.001] (N = 20; n = 4, ROIs = 5/animal) and arteries [F(147,49) = 1.66, p = 0.01] (N = 20; n = 4, ROIs = 5/animal). At 2.5min post cocaine, it decreased 5.16 ± 1.9% (n = 4) from 41.34 ± 8.1 μm to 38.8 ± 8.5 μm in veins and 4.37 ± 1.1% (n = 4) from 25.8 ± 4.1 μm to 22.6 ± 4.4 μm in arteries (Fig. 3a). However, in the awake state the vessel diameter changes were not significant for neither veins [F(147,49) = 0.89, p = 0.68] (0.8 ± 3.2%, n = 4) nor arteries [F(147,49) = 0.95, p = 0.56](-0.77 ± 4.0, n = 4) (Fig. 3b).

3.3. Cocaine decreased CBFv and HbO_2 in anesthetized but not in awake animals

As hypothesized, the vasodilation induced by isoflurane affected the hemodynamic responses to acute cocaine. Fig. 4a shows CBFv maps at baseline (e.g., t = 0min) and t = 25min after cocaine in the awake (a_0 & a_1) and anesthetized (a_3 & a_4) states. Fig. 4b_1 and c_1 show the time courses of CBFv and HbO_2 changes in arteries, veins and cortical tissue in awake (solid green) and isoflurane (solid orange) conditions. A two-way repeated measure ANOVA showed a significant interaction between consciousness state and time (post injection) in CBFv [F(34, 102) = 2.58, p < 0.001]. The CBFv decrease after cocaine was significantly larger in anesthetized than in awake mice (Fig. 4b_1). One way repeated ANOVAs for cocaine-induced CBFv changes run separately for the awake and anesthetized states showed that the effects of cocaine on CBFv were not significant in the awake state [F(34,102) = 1.51, p = 0.06], whereas CBFv decreased significantly in the anesthetized mice [F(34,102) = 5.66, p < 0.001]. Multiple comparisons showed that CBFv was significantly reduced at 3–30 min post cocaine in the anesthetized mice. Comparison of cocaine-induced CBFv changes (ΔCBFv) between the anesthetized (−14.9 ± 4.9%) and the awake (5.75 ± 6.3%) states was significant (n = 4, t = 2.57, p = 0.04) (Fig. 4b_2).

Cocaine caused a significant decrease in ΔHbO_2 in the anesthetized but not in the awake state (Fig. 4c_1). A two-way repeated ANOVA found a significant interaction between consciousness state and post-injection [F(34,102) = 3.17, p < 0.001]. Multiple comparisons found that relative to the awake state, anesthetized animals showed a significant decrease at 6, 7, and 11–30 min post injection. This pattern was similar to that of ΔCBFv, with the differences being most pronounced 10–30min post injection. Separate one-way repeated ANOVA showed that for the awake condition cocaine did not change ΔHbO_2 relative to baseline [F(34,102) = 0.76, p = 0.82], whereas in the anesthetized state cocaine decreased ΔHbO_2 [F(34,102) = 8.35, p < 0.001]. Multiple comparisons in the anesthetized animals showed that ΔHbO_2 was decreased below baseline from 2 to 30 min post injection (Fig. 4c_1). Fig. 4c_2 shows that ΔHbO_2 in the anesthetized state (i.e., −5.11 ± 0.82%, n = 4) differed significantly from that in the awake state (0.36 ± 1.83%, t = 2.72, p = 0.03).

We also assessed the correlations between ΔHbO_2 and ΔCBFv for the anesthetized and the awake states from 5 min before to 10 min after cocaine administration. There was a significant positive correlation between ΔHbO_2 and ΔCBFv in the anesthetized (R(899) = 0.90 ± 0.26, p < 0.001) (Fig. 4d_1) and in the awake states (R(899) = 0.61 ± 0.35, p < 0.001) (Fig. 4d_2). These results indicate the close relationship between ΔHbO_2 and ΔCBFv responses to cocaine and that this relationship is conserved under anesthesia despite the enhancement of cocaine's effect. Furthermore, this data supports the hypothesis that cocaine-induced reduction in cerebral blood flow induces the reduced tissue oxygenation observed in the cerebral cortex.

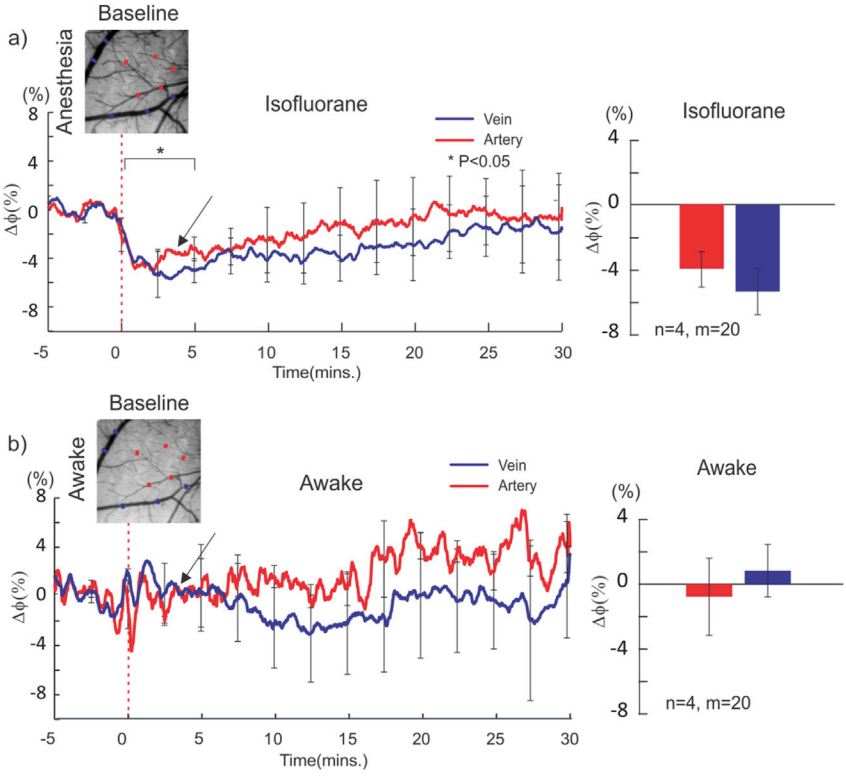

Fig. 3. Cocaine effects on constriction of veins and arteries in the awake and anesthetized states. **a)** Cocaine-induced constriction of veins and arteries in the anesthetized state, with a maximal decrease of 4.37 ± 1.1% in arteries [F(147,49) = 1.66, p = 0.01] and of 5.16 ± 1.9% in veins [F(147,49) = 3.39, p < 0.001] occurring at ~3min after cocaine, both of which recovered gradually. **b)** In the awake state, there were no significant vasoconstriction in arteries (−0.77 ± 4.0% [F(147,49) = 0.95, p = 0.56] and in veins (0.8 ± 3.2% [F(147,49) = 0.89, p = 0.68]) after cocaine.

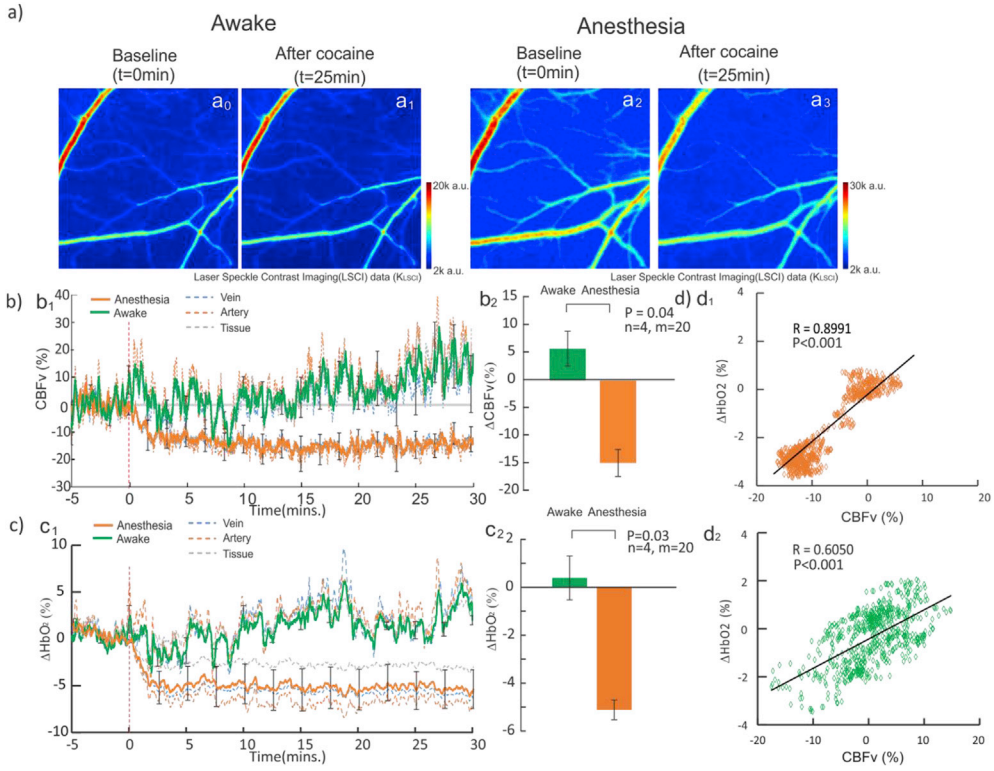

Fig. 4. Cocaine-induced ΔCBFv and ΔHbO_2 in the awake and isoflurane anesthetized states. **a)** Images to show CBFv difference between baseline (t = 0min) and after cocaine (t = 25min) in the awake (**a_0-a_1**) and anesthetized states (**a_2-a_3**). **b_1)** ΔCBFv rapidly decreased −13.2 ± 13.5% at ~3min post cocaine and remained low in the anesthetized state (orange line) [F(34,102) = 5.66, p < 0.001], but showed no significant change [F=(34,102) = 1.51, p = 0.06] in the awake state (green line). **b_2)** Cocaine-induced mean ΔCBFv in the awake and anesthetized states were significantly different (p = 0.04). **c_1)** ΔHbO_2 rapidly decreased −5.11 ± 1.83% at ~3min post cocaine and remained low [F(34,102) = 8.35, p < 0.001] in the anesthetized state, but showed no significant change in the awake state [F(34,102) = 0.76, P = 0.82]. **c_2)** Cocaine-induced mean ΔHbO_2 in the awake and anesthetized states were significantly different (p = 0.03). **d)** ΔHbO_2 and ΔCBFv showed strong positive correlation with R(899) = 0.90 (p < 0.001) in the anesthetized state and R(899) = 0.61 (p < 0.001) in the awake state during t = −5 to 10min.

3.4. *Cocaine affected neuronal $[Ca^{2+}]_i$ in the awake and anesthetized states*

Fig. 5a_0-a_1 and b_0-b_1 show images of intracellular neuronal calcium ($[Ca^{2+}]_i$ fluorescence from the somatosensory cortex before and after cocaine, respectively. Fig. 5a_2 is the ratio image of Fig. 5a_1 (t = 3min after cocaine) over Fig. 5a_0 (t = 0 min, baseline) from an awake animal, Fig. 5b_2 is the ratio image from an anesthetized animal. Fig. 5a_3&b_3 are the time course $[Ca^{2+}]_i$ fluorescence intensity change (i.e. ΔF(t)/F %) in the selected ROIs (e.g., dashed circles in Fig. 5a_2&b_2) in the awake and anesthetized conditions, showing that after cocaine the mean $[Ca^{2+}]_i$ in the cortex (solid lines) did not change in the awake animal but increased in the anesthetized animal. Statistical results across groups are summarized in Fig. 5a_4&5b_4. In the awake condition, $[Ca^{2+}]_i$ averaged over 5 min before and after cocaine (dashed boxes in Fig. 5a_3) shows a nonsignificant decrease over its background from 0.26 ± 0.38% at baseline (averaged over 5min before cocaine) to −0.72 ± 1.32% after cocaine, and the difference was not significant (repeat measure ANOVA [F(14,28) = 1.1, p = 0.39], n = 3) (Fig. 5a_4). In the anesthetized state, however, $[Ca^{2+}]_i$ fluorescence increased significantly from 0.07 ± 0.07% at baseline to 1.86 ± 0.15% after cocaine [F(14,56) = 8.16, p < 0.001, n = 5] (Fig. 5b_4). Multiple comparison showed 1.82 ± 0.31% $[Ca^{2+}]_i$ increase after cocaine (t = 5min, p = 0.003).

The fast fluorescence variations observed in awake animals (Fig. 5a_3) correspond to Ca^{2+} spikes that reflected synchronized neuronal activities within the selected ROI (e.g., red circle in Fig. 5a_2). For awake animals, the dashed boxes in Fig. 5.a_3 show no significant difference in neuronal mean $[Ca^{2+}]_i$ fluorescence between baseline (averaged over 5min before

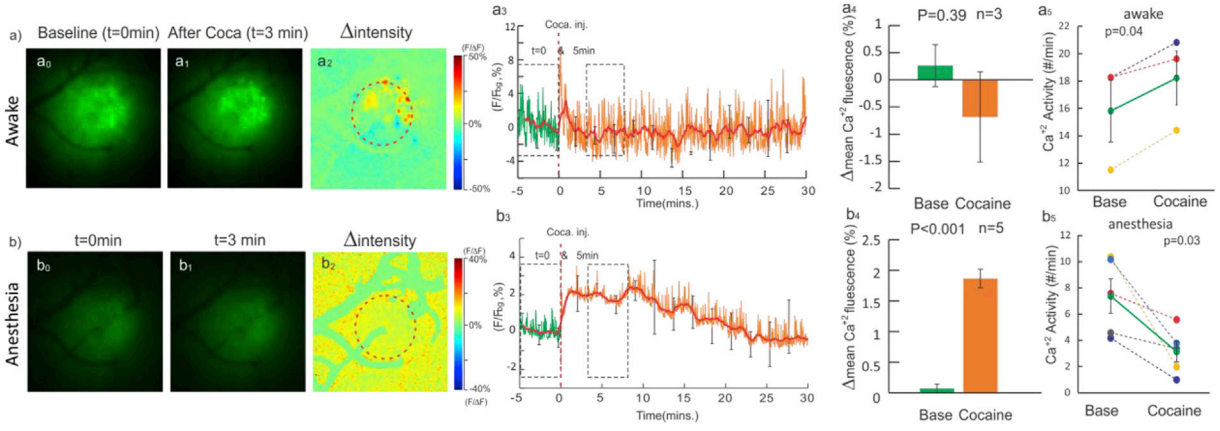

Fig. 5. Cocaine-induced neuronal $[Ca^{2+}]_i$ changes in the awake and anesthetized states. **a_0-a_3)** and **b_0-b_3)** Ca^{2+} fluorescence images before and after cocaine and their ratio images in the awake and anesthetized states. **a_3-b_3)** Time-lapse $\Delta[Ca^{2+}]_i$ (%) in the awake and anesthetized states. **a_4-b_4)** $[Ca^{2+}]_i$ differences before (t = 0min) and after (t = 5min) cocaine were non significant in the awake state [F(14,28) = 1.1, p = 0.39], but increased 1.86 ± 0.15% [F(14,56) = 8.16, p < 0.001, n = 5] in the anesthetized state. **a_5-b_5)** Ca^{2+} activities averaged over 5min before and after cocaine, which increased from 15.8 ± 5.3 count/min to 18.2 ± 3.2 count/min (p = 0.04) after cocaine in the awake state but decreased from 7.4 ± 2.9 count/min to 3.16 ± 1.7 count/min (p = 0.03) in the anesthetized state.

cocaine) and after cocaine, but the frequency of $[Ca^{2+}]_i$ activities averaged over 5min increased significantly from 15.8 ± 5.3 count/min at baseline to 18.2 ± 3.2 count/min after cocaine ($p = 0.04$). For anesthetized animals, there was a significant increase in mean $[Ca^{2+}]_i$ fluorescence after cocaine (Fig. 5b$_4$), but the frequency of $[Ca^{2+}]_i$ activities decreased significantly from 7.4 ± 2.9 count/min at baseline to 3.16 ± 1.7 count/min after cocaine ($p = 0.03$). Summarizing, in anesthetized animals, cocaine increased neuronal intracellular $[Ca^{2+}]_i$ accumulation but decreased neuronal Ca^{2+} transient activity whereas in awake animals, cocaine did not change neuronal intracellular $[Ca^{2+}]_i$ accumulation but increased neuronal Ca^{2+} transient activity.

3.5. Cocaine increased neuronal $[Ca^{2+}]_i$ transients in awake animals

Neuronal Ca^{2+} fluorescence in brain was much higher in the awake than in the anesthetized state (i.e., ~32.9% higher, Fig. 2c above), which allowed us to detect Ca^{2+} transients from individual neurons in the awake condition (e.g., bright spots in Fig. 5d$_2$), but not in the anesthetized state. To characterize cellular neuronal activities before and after cocaine, we applied 80 Hz fluorescence image acquisition to capture $[Ca^{2+}]_i$ transients ($\Delta F_i(t)/F$) from individual neurons within a large field of view. Background subtraction was applied to enhance visualization of individual neuronal activity (Fig. 6a) and accurately count the number of activated neurons in each frame. Fig. 6b shows that the average active neuron counts were 52 per frame at baseline and increased to 99 neurons at 2.4 min after cocaine (high status pointed at Fig. 6a&b).

In parallel, short-term Fourier transform (STFT) analysis revealed that cocaine increased neuronal activity in the awake state (Fig. 6c), which is in agreement with the increased frequency of neuronal Ca^{2+} transients in Fig. 5a$_5$ above. The power spectral density (PSD) used to quantify neuronal activation peaked at ~0.5 with a central frequency ~0.15 Hz before cocaine, but it increased to ~1.62 with a peak frequency at ~0.09 Hz after cocaine (Fig. 6d). The bandwidth of PSD analyzed with Gaussian fitting (green lines, Fig. 6d) decreased from ~0.12 Hz at baseline to ~0.08 Hz after cocaine (Fig. 6d$_1$&d$_2$). Statistical analyses showed that cocaine increased PSD ($n = 5$, $p = 0.02$) and decreased both the bandwidth (Fig. 6e$_1$ $n = 5$, $p < 0.001$) and the central frequencies of neuronal activation (Fig. 6e$_2$, $n = 5$, $p = 0.03$).

Additionally, cocaine enhanced the synchronization of neuronal activities based on the quantification of the correlation between individual neurons. As illustrated in Fig. 6f, 10 neurons (1–10 in Fig. 6a) were randomly selected to dynamically track their $\Delta F(t)$ at baseline and after cocaine. $\Delta F(t)$ spikes in these neurons were random and not coordinated temporally with each other before cocaine ($t < 0$min); after cocaine ($t = 1$min), they became more active and synchronized. Fig. 6g shows the correlation coefficient between the neuronal activities significantly increased from 0.37 ± 0.08 at baseline to 0.51 ± 0.1 after cocaine [$F(4,9) = 7.84$, $p = 0.04$, $n = 5$ mice] (Fig. 6h).

4. Conclusion and discussion

In this study we examined the effect of isoflurane anesthesia on cerebral vasculature, hemodynamics, and mean intracellular $[Ca^{2+}]_i$ fluorescence ($\overline{F}$) and $[Ca^{2+}]_i$ transients ($\Delta F/F$) from neuronal populations in mouse cortex compared to the awake state. We also compared the effects of acute cocaine between the awake and anesthetized conditions and showed significant effects of anesthesia on cocaine effects. At baseline isoflurane induced dilation of veins and arteries and increased CBFv,

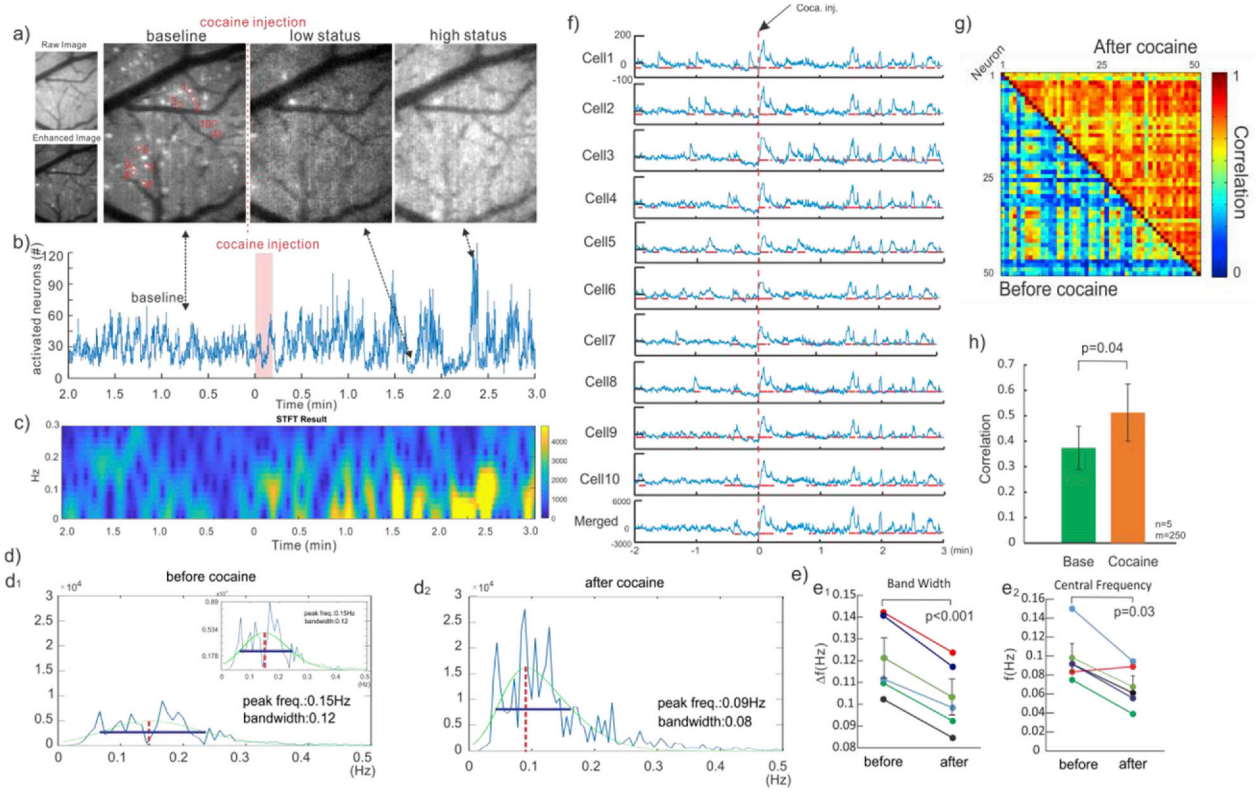

Fig. 6. Enhanced $[Ca^{2+}]_i$ activities of individual neurons and their synchronization after cocaine in the awake state. **a)** GCaMP expression of individual neurons in the cortex (FOV: 0.5×0.6 mm^2). **b)** The counts of activated neurons to represent their activities with time, showing increased firing synchronization after cocaine. **c)** STFT graph to show frequencies of the firing neurons, which enhanced synchronization of activities within the 0.07 Hz range. **d)** The bandwidth of neuron cell firing frequencies (via FFT) was narrowed ($p < 0.001$) and peak frequency decreased ($p = 0.03$) after cocaine. **e)** Tracking of 50 activated cells and their activities. **f)** Activities randomly selected from 10 of the 50 neurons, showing enhanced temporal correlation (synchronization). Red lines: cells with ≥5% increase in activation period in each trace. **g)** Color map representing the correlation between the activities of individual neurons before and after cocaine (Blue: low correlation, Red: High correlation). **h)** The correlation coefficients among individual neurons increased from 0.37 ± 0.08 before cocaine to 0.51 ± 0.1 after cocaine [$F(4,9) = 7.84$, $p = 0.04$].

while simultaneously depressing neuronal activity as measured by mean $[Ca^{2+}]_i$ fluorescence intensity and $[Ca^{2+}]_i$ transients (corresponding to average activities across neurons in the field of view). When cocaine was given in the anesthetized state it triggered vasoconstriction of veins and arteries and reduced CBFv; whereas these hemodynamic changes were not observed when cocaine was given in the awake state. Additionally, in the anesthetized but not in the awake state, cocaine increased mean $[Ca^{2+}]_i$ fluorescence. However, analyses of cocaine's effects in the awake state revealed that it increased $[Ca^{2+}]_i$ transients in neuronal populations and it increased the number of neurons that showed $[Ca^{2+}]_i$ transients. The enhanced neuronal activation by cocaine in awake animals but not anesthetized is consistent with prior findings from Koulchitsky et al. (2012) who reported that cocaine increased the firing of dopamine (DA) neurons in awake animals whereas it decreased DA neuron firing in anesthetized animals. Analyses of individual neuronal $[Ca^{2+}]_i$ transients showed that cocaine also increased neuronal activity synchronization (measured by $\Delta F(t)/F$) in the awake mice. Unfortunately, under isoflurane anesthesia individual neuronal transients were not detectable so we could not assess if cocaine affected synchronization of neuronal activities in anesthetized animals.

Isoflurane dilated cerebral veins and arteries and increased CBFv relative to the awake state, which is consistent with studies showing that isoflurane relaxes smooth muscles within vessel walls causing dilation (Iida et al., 1998). The observed dilation was larger in arteries than in veins likely due to more muscular structures in their vessel walls. As expected from the observed vasodilation, isoflurane also increased CBFv (Timothy, 2007). Isoflurane also depressed Ca^{2+} signaling, consistent with inhibition of neuronal activity during isoflurane's anesthesia (Wu et al., 2016), which is also in agreement with prior studies showing that isoflurane inhibited neuronal activities (Baumgart et al., 2015, Study, 1994).

The hemodynamic and neuronal effects of cocaine were also profoundly affected by isoflurane anesthesia. In the anesthetized state, cocaine significantly decreased CBFv and HbO_2 - an effect observable 3 min post injection that persisted throughout the 30-min post cocaine measurement. In contrast in the awake state cocaine did not change CBFv and HbO_2. This is consistent with our prior reports of cocaine-induced vasoconstriction and CBFv reduction in the anesthetized mouse brain (Ren et al., 2012; Allen et al., 2018), which occurred promptly post cocaine injection in this study and sustained for at least 30 min (Liu et al., 1993). Similarly, cocaine-induced ΔHbO_2 decreases in the anesthetized state are consistent in magnitude and dynamics with those we reported previously in anesthetized animals (Du et al., 2018). In contrast, in the awake state, cocaine did not change vessel diameter or hemodynamics until 15 min post cocaine at which time it increased $\Delta CBFv$ and ΔHbO_2. Several factors could contribute to the differences between awake and anesthetized states. First, because isoflurane dilates blood vessels this would make cocaine-induced vasoconstriction more detectable. Second, there could be an interaction between isoflurane and cocaine at the vascular and/or neuronal level. Indeed, Tsukada et al. reported that in non-human primates isoflurane enhanced cocaine's inhibitory effects at the dopamine transporter (Tsukada et al., 1999) and we reported that in rodents isoflurane affected the binding of cocaine to the dopamine transporter (Du et al., 2009). Finally, awake mice may have additional effects that buffer the acute vasoconstriction. For instance, while vasoconstriction from cocaine would decrease CBF, the increases in neuronal activity triggered by cocaine in the awake state would increase it, which would drive vasodilation of the vasoconstricted vessels. In contrast in the anesthetized state the inhibition of neuronal activity by isoflurane would blunt the neuronal activation by cocaine, which would further contribute to CBF decreases. Since cocaine-induced vasoconstriction has been observed in isolated vessel segments (Egashira et al., 1991, El-Fawal and Wood, 1995) in the absence of any anesthesia, it is likely that the neuronal activating effects of cocaine (and presumably associated engagement of astrocytes involved in neurovascular coupling) might have counteracted the vasoconstricting effects of acute cocaine when given in the awake state to naïve animals. However, in preclinical models of chronic cocaine given in the awake state and in clinical studies in cocaine abusers there is clear evidence of marked vasoconstriction of cerebral vessels, reductions in CBF and ischemia (You et al., 2017; Volkow et al., 1988). These differences suggest that while acute cocaine in the awake state might not trigger cerebral vessel vasoconstriction in a naïve animal, with repeated exposures the hemodynamic effects of cocaine might become sensitized as shown by our prior studies (Ren et al., 2012). Alternatively, the neuronal activating effects of cocaine might decrease with repeated exposure and thus be less able to counterbalance cocaine's vasoconstricting effects. Indeed, we have documented that there is a marked attenuation of cocaine's enhancement of dopaminergic signaling in the brain both in chronic animal models (Park et al., 2013) and in cocaine abusers (Volkow et al., 2014).

In parallel, cocaine induced Ca^{2+} fluorescence responses including mean $[Ca^{2+}]_i$ fluorescence ($\bar{F}$) and $[Ca^{2+}]_i$ transient changes over the baseline (before cocaine) were different in the anesthetized and awake conditions. In anesthetized state, mean $[Ca^{2+}]_i$ fluorescence increased after cocaine, whereas it did not change in the awake state. The differences might reflect the fact that isoflurane inhibits Ca^{2+} channels in neurons reducing individual neuron's $[Ca^{2+}]_i$ changes (Orestes et al., 2009). Additionally, in anesthetized animals isoflurane triggered internal Ca^{2+} release via its effects in ryanodine receptors (RyR) redox modification, extracellular signal regulated kinases (ERK) and cAMP/Ca^{2+} response element binding protein (CREB) phosphorylation (Hidalgo and Núñez, 2007), which might underlie the increase in mean $[Ca^{2+}]_i$ observed in the isoflurane anesthetized animals. In the awake state, although mean $[Ca^{2+}]_i$ fluorescence did not change after cocaine, neuronal $[Ca^{2+}]_i$ transients increased and the activities among neurons became more synchronized.

The integration of GCaMP expression with our MIP allowed us to image individual neuronal activity in the awake state, though it lacked the sensitivity to detect the markedly weakened neuronal activity in the anesthetized state. Before cocaine, the individual neuronal transients ($\Delta F(t)/F$) occurred randomly with low synchronization between neurons. However, after cocaine, activities between individual neurons were more synchronized, which was reflected in an increase in the correlation coefficients between neuronal activities compared to baseline. To quantify the synchronization of neuronal activity, activated cell numbers in time course were processed via FFT and STFT. The analysis in frequency domain showed that cocaine enhanced neuronal activities in the low frequency range of ~0.07 Hz and that it reduced the activation frequency bandwidth from 0.12 ± 0.02 Hz at baseline to 0.1 ± 0.01 Hz post cocaine ($n = 5$, Fig. 6e1) while shifting the central frequency from 0.10 ± 0.03 Hz to 0.07 ± 0.02 Hz ($n = 5$, Fig. 6e2), consistent with an enhanced synchronization of neuronal activities by cocaine. This is reminiscent of the enhanced synchronization in slow frequency neuronal activity we recently reported when acute cocaine was given to animals that had been given chronic cocaine in the awake state but imaged during anesthesia (Chen et al., 2018). In the chronic cocaine exposed animals, we showed that acute cocaine decreased high frequency local field potentials (LFP) while it increased synchronization of slow LFP and hemodynamics in the somatosensory cortex. We interpret the enhanced synchronization of neuronal activity to reflect the catecholaminergic effects of cocaine, which would reduce the randomness of background neuronal firing rates (Du et al., 2006).

The apparent paradoxical finding in the awake animals showing that acute cocaine enhanced neuronal activities while not affecting CBFv is consistent with our findings that cocaine disrupted neurovascular coupling, which we had shown in anesthetized animals (Chen et al., 2016a,b). Thus this finding indicates that cocaine induced neurovascular uncoupling also occurs in the awake state. However, since the hemodynamic measures were obtained over larger cortical areas than those for the neuronal $[Ca^{2+}]_i$ measures we can not rule out the possibility that the relatively large ROI and the compartment-mixed quantification (veins,

arteries, tissue) of hemodynamics (Fig. 4) might have washed out the local neuronal responses (Fig. 6).

We measured CBFv in the vessels and within the brain tissue using a method based on the Doppler shift of particles (e.g., red blood cells) or speckle variation (Luo et al., 2008). The slower recovery of CBFv (Fig. 4) than vessel diameters (Fig. 3) observed in the anesthetized animals might reflect other physiological factors affecting CBFv including changes in blood pressure, pulse, cardiac efficiency and stroke volume (Mayet and Hughes, 2003). We hypothesize that the reductions in CBFv from acute cocaine would eventually recover but documenting this would have required a longer period of imaging than the 30min we used in our study.

A limitation in our study was that the recordings in the awake condition preceded those in the anesthetized state but we showed that CBFv returned to baseline after interruption of isoflurane indicating that the CBFv differences between awake and anesthetized conditions were not due to the order of the condition. However, we can not rule out the confound from having received the first cocaine dose in the awake state versus having received a second cocaine dose under anesthesia. Note that to minimize the effects from one state to the other we sustained each state for a long period (e.g., 1 h), which allowed for physiological stabilization of the animals under each condition. Though we trained animals prior to awake imaging to minimize stress effects from a novel situation and at the time of imaging mice did not show classical signs of stress (vocalization, amounts of fecal matter excreted or stress-induced diarrhea and level of motion) we can not completely rule out confounds due to stress in our findings (Kislin et al., 2014; Madularu et al., 2017).

In summary, the effects of cocaine in the brain during the anesthetized state (using isoflurane) differed from those observed in the awake condition. Isoflurane dilated vessels and depressed neuronal Ca^{2+} activity, confounding cocaine's hemodynamic and neuronal effects on the brain. Using a novel strategy for optical imaging of awake mice we observed that while acute cocaine did not change hemodynamics in the cortex it significantly increased neuronal activities and neuronal synchronization in the awake state. These findings indicate that the anesthetic agents (e.g., isoflurane) interact with the pharmacological effects of cocaine in brain highlighting the importance of conducting preclinical studies on the effects of cocaine in the brain of awake animals.

Conflicts of interest

The authors declare no competing financial interests.

Acknowledgments

We thank Kevin Clare for the help on building mobile cage and imaging. This research was supported in part by grants R01DA029718 (C.D., Y.P.), R21DA042597(Y.P., C.D.) from the National Institutes of Health. The authors would also like to thank the NIDA drug supply program for providing the cocaine used in this study.

Appendix A. Supplementary data

Supplementary data to this article can be found online at https://doi.org/10.1016/j.neuroimage.2018.11.062.

References

Allen, C.P., Park, K., Li, A., Volkow, N.D., Koob, G.F., Pan, Y., Hu, X., Du, C., 2018. Enhanced neuronal and blunted hemodynamic reactivity to cocaine in the prefrontal cortex following extended cocaine access: optical imaging study in anesthetized rats. Addict. Biol. https://doi.org/10.1111/adb.12615.

Baumgart, J.P., Zhou, Z.Y., Hara, M., Cook, D.C., Hoppa, M.B., Ryan, T.A., Hemmings, H.C., 2015. Isoflurane inhibits synaptic vesicle exocytosis through reduced Ca^{2+} influx, not Ca^{2+}-exocytosis coupling. PNAS 112, 11959–11964.

Center for Behavioral Health, 2016. Statistics and Quality.

Chen, W., Liu, P., Volkow, N.D., Pan, Y., Du, C., 2016a. Cocaine attenuates blood flow but not neuronal responses to stimulation while preserving neurovascular coupling for resting brain activity. Mol. Psychiatr. 21 (10), 1408–1416.

Chen, W., Volkow, N.D., Li, J., Pan, Y., Du, C., 2018. Cocaine decreases spontaneous neuronal activity and increases low-frequency neuronal and hemodynamic cortical oscillations. Cereb. Cortex bhy057, 1–13.

Chen, T.W., Wardill, T.J., Sun, Y., Pulver, S.R., Renninger, S.L., Baohan, A., Schreiter, E.R., Kerr, R.A., Orger, M.B., Jayaraman, V., Looger, L.L., Svoboda, K., Kim, D.S., 2013. Ultra-sensitive fluorescent proteins for imaging neuronal activity. Nature 499, 295–300.

Chen, W., Park, K., Volkow, N.D., Pan, Y.T., Du, C.W., 2016b. Cocaine-induced abnormal cerebral hemodynamic responses to forepaw stimulation assessed by integrated multi-wavelength spectroimaging and laser speckle contrast imaging. IEEE J. Sel. Top. Quant. Electron. 22, 6802608.

Desai, R., Patel, U., Rupareliya, C., Singh, S., Shah, M., Patel, R.S., Patel, S., Mahuwala, Z., 2017. Impact of cocaine use on acute ischemic stroke patients: insights from nationwide inpatient sample in the United States. Cureus 9 (8), e1536.

Dombeck, D.A., Khabbaz, A.N., Collman, F., Adelman, T.L., Tank, D.W., 2007. Imaging large-scale neural activity with cellular resolution in awake, mobile mice. Neuron 56 (1), 43–57.

Du, C., Tully, M., Volkow, N.D., Schiffer, W.K., Yu, M., Luo, Z., Koretsky, A.P., Benveniste, H., 2009. Differential effects of anesthetics on cocaine's pharmacokinetic and pharmacodynamic effects in brain. Eur. J. Neurosci. 30, 1565–1575.

Du, C., Yu, M., Volkow, N.D., Koretsky, A.P., Fowler, J.S., Benveniste, H., 2006. Cocaine increases the intracellular calcium concentration in brain independently of its cerebrovascular effects. J. Neurosci. 26 (45), 11522–11531.

Du, C., Volkow, N.D., You, J., Park, K., Allen, C.P., Koob, G.F., Pan, Y., 2018 Oct 3. Cocaine-induced ischemia in prefrontal cortex is associated with escalation of cocaine intake in rodents. Mol. Psychiatr.

Dunn, A.K., Devor, A., Bolay, H., Andermann, M.L., Moskowitz, M.A., Dale, A.M., Boas, D.A., 2003. Simultaneous imaging of total cerebral hemoglobin concentration, oxygenation, and blood flow during functional activation. Opt. Lett. 28 (1), 28–30.

Dunn, A.K., Devor, A., Dale, A.M., Boas, D.A., 2005. Spatial extent of oxygen metabolism and hemodynamic changes during functional activation of the rat somatosensory cortex. Neuroimage 27 (2), 279–290.

Egashira, K., Morgan, K.G., Morgan, J.P., 1991. Effects of cocaine on excitation-contraction coupling of aortic smooth muscle from the ferret. J. Clin. Invest. 87, 1322–1328.

El-Fawal, H.A., Wood, R.W., 1995. Airway smooth muscle relaxant effects of the cocaine pyrolysis product, methylecgonidine. J. Pharmacol. Exp. Therapeut. 272, 991–996.

Goldey, G.J., Roumis, D.K., Glickfeld, L.L., Kerlin, A.M., Reid, R.C., Bonin, V., Schafer, D.P., Andermann, M.L., 2014. Removable cranial windows for long-term imaging in awake mice. Nat. Protoc. 9, 2515–2538.

Gu, X., Chen, W., You, J., Koretsky, A.P., Volkow, N.D., Pan, Y., Du, C., 2018. Long-term optical imaging of neurovascular coupling in mouse cortex using GCaMP6f and intrinsic hemodynamic signals. Neuroimage 165, 251–264.

Hidalgo, C., Núñez, M.T., 2007. Calcium, iron and neuronal function. UBMB Life 59, 280–285.

Iida, H., Ohata, H., Iida, M., Watanabe, Y., Dohi, S., 1998. Isoflurane and sevoflurane induce vasodilation of cerebral vessels via ATP-sensitive K+ channel activation. Anesthesiology 89, 954–960.

Jacques, S.L., 2013. Optical properties of biological tissues: a review. Phys. Med. Biol. 58, R37–R61.

Kislin, M., Mugantseva, E., Molotkov, D., Kulesskaya, N., Khirug, S., Kirilkin, I., Pryazhnikov, E., Kolikova, J., Toptunov, D., Yuryev, M., Giniatullin, R., Voikar, V., Rivera, C., Rauvala, H., Khiroug, L., 2014. Flat-floored air-lifted platform: a new method for combining behavior with microscopy or electrophysiology on awake freely moving rodents. J. Vis. Exp. 88, e51869.

Koulchitsky, S., De Backer, B., Quertemont, E., Charlier, C., Seutin, V., 2012. Differential effects of cocaine on dopamine neuron firing in awake and anesthetized rats. Neuropsychopharmacology 37 (7), 1559–1571.

Kufahl, P.R., Pentkowski, N.S., Heintzelman, K., Neisewander, J.L., 2009. Cocaine-induced Fos expression is detectable in the frontal cortex and striatum of rats under isoflurane but not α-chloralose anesthesia: implications for FMRI. J. Neurosci. Methods 181, 241–248.

Lin, M.Z., Schnitzer, M.J., 2016. Genetically encoded indicators of neuronal activity. Nat. Neurosci. 19, 1142–1153.

Liu, C.P., Tunin, C., Kass, D.A., 1993. Transient time course of cocaine-induced cardiac depression versus sustained peripheral vasoconstriction. J. Am. Coll. Cardiol. 21, 260–268.

Luo, Z., Wang, Z., Yuan, Z., Du, C., Pan, Y., 2008. Optical coherence Doppler tomography quantifies laser speckle contrast imaging for blood flow imaging in the rat cerebral cortex. Opt. Lett. 33 (10), 1156–1158.

Luo, Z., Yuan, Z., Pan, Y., Du, C., 2009 May 1. Simultaneous imaging of cortical hemodynamics and blood oxygenation change during cerebral ischemia using dual-wavelength laser speckle contrast imaging. Opt. Lett. 34 (9), 1480–1482.

Madularu, D., Mathieu, A.P., Kumaragamage, C., Reynolds, L.M., Near, J., Flores, C., Rajah, M.N., 2017. A non-invasive restraining system for awake mouse imaging. J. Neurosci. Methods 287, 53–57.

Mayet, J., Hughes, A., 2003. Cardiac and vascular pathophysiology in hypertension. Heart 89 (9), 1104–1109.

Orestes, P., Bojadzic, D., Chow, R.M., Todorovic, S.M., 2009. Mechanisms and functional significance of inhibition of neuronal T-Type calcium channels by isoflurane. Mol. Pharmacol. 75, 542–554.

Park, K., Volkow, N.D., Pan, Y., Du, C., 2013. Chronic cocaine dampens dopamine signaling during cocaine intoxication and unbalances D1 over D2 receptor signaling. J. Neurosci. 33 (40), 15827–15836.

Park, K., You, J., Du, C., Pan, Y., 2015. Cranial window implantation on mouse cortex to study microvascular change induced by cocaine. Quant. Imag. Med. Surg. 5, 97–107.

Ren, H., Du, C., Yuan, Z., Park, K., Volkow, N.D., Pan, Y., 2012. Cocaine-induced cortical microischemia in the rodent brain: clinical implications. Mol. Psychiatr. 17, 1017–1025.
Study, R.E., 1994. Isoflurane inhibits multiple voltage-gated calcium currents in hippocampal pyramidal neurons. Anesthesiology 81, 104–116.
Timothy, Q., 2007. Duong Cerebral blood flow and BOLD fMRI responses to hypoxia in awake and anesthetized rats. Brain Res. 1135, 186–194.
Tran, C.H., Gordon, G.R., 2015. Acute two-photon imaging of the neurovascular unit in the cortex of active mice. Front. Cell. Neurosci. 9–11.
Treadwell, S.D., Robinson, T.G., 2007. Cocaine use and stroke. Postgrad. Med. J. 83, 389–394.
Tsukada, H., Nishiyama, S., Kakiuchi, T., Ohba, H., Sato, K., Harada, N., Nakanishi, S., 1999. Isoflurane anesthesia enhances the inhibitory effects of cocaine and GBR12909 on dopamine transporter: PET studies in combination with microdialysis in the monkey brain. Brain Res. 849, 85–96.
Volkow, N.D., Mullani, N., Gould, K.L., Adler, S., Krajewski, K., 1988. Cerebral blood flow in chronic cocaine users: a study with positron emission tomography. Br. J. Psychiatry 152, 641–648.
Volkow, N.D., Tomasi, D., Wang, G.J., Logan, J., Alexoff, D.L., Jayne, M., Fowler, J.S., Wong, C., Yin, P., Du, C., 2014. Stimulant-induced dopamine increases are markedly blunted in active cocaine abusers. Mol. Psychiatr. 19 (9), 1037–1043.
Wu, T.L., Mishra, A., Wang, F., Yang, P.F., Gore, J.C., Min, L.C., 2016. Effects of isoflurane anesthesia on resting-state fMRI signals and functional connectivity within primary somatosensory cortex of monkeys. Brain Behav. 6, e00591.
You, J., Volkow, N.D., Park, K., Zhang, Q., Clare, K., Du, C., Pan, Y., 2017. Cerebrovascular adaptations to cocaine-induced transient ischemic attacks in the rodent brain. JCI Insight 2, e90809.
Yuan, Z., Luo, Z., Volkow, N.D., Pan, Y., Du, C., 2011. Imaging separation of neuronal from vascular effects of cocaine on rat cortical brain in vivo. Neuroimage 54 (2), 1130–1139.
Zhang, Q., You, J., Volkow, N.N., Choi, J., Yin, W., Wang, W., Pan, Y., Du, C., 2016. Chronic cocaine disrupts neurovascular networks and cerebral function: optical imaging studies in rodents. J. Biomed. Optic. 21 (2), 26006.